environmental sciences proceedings

MDPI

Proceeding Paper

Wind Energy Calculations of a 15 MW Floating Wind Turbine System in the Mediterranean Sea †

Thomas P. Mazarakos

Naval Architecture Department, School of Engineering, University of West Attica, Campus 1, Ag. Spyridonos 28, 12241 Egaleo, Greece; tmazar@uniwa.gr; Tel.: +30-2105385367

† Presented at the 16th International Conference on Meteorology, Climatology and Atmospheric Physics—COMECAP 2023, Athens, Greece, 25–29 September 2023.

Abstract: This study examines how a floating wind turbine responds to irregular waves. It gives a detailed explanation of the floating body's geometrical features as well as the outcomes in terms of the incident waves. A discussion of the system's modeling in detail is followed by the presentation of numerical results in the frequency domain. The floating structure, which is exposed to the action of regular and irregular waves in finite-depth waters, encompasses a semi-submersible offshore floating structure, moored with conventional catenary mooring lines, supporting a 15 MW Wind Turbine. The analysis's objective is to determine which sea states produce the significant and maximum first-order forces of the offshore structure, due to operating wave conditions, obtained through wave hindcast time series in the Mediterranean Sea. Finally, the annual energy output of the 15 MW Wind Turbine is presented.

Keywords: renewable energy; offshore structures; mooring systems; wind energy; wave; wind; environment

check for updates

Citation: Mazarakos, T.P. Wind Energy Calculations of a 15 MW Floating Wind Turbine System in the Mediterranean Sea. *Environ. Sci. Proc.* **2023**, *26*, 191. https://doi.org/10.3390/environsciproc2023026191

Academic Editors: Konstantinos Moustris and Panagiotis Nastos

Published: 15 September 2023

1. Introduction

In recent years, the lack of energy sources has become a primary issue. This makes the need for renewable energy more pressing than ever. As global warming increases due to increasing CO_2 emissions, there is a gradual shift away from fossil fuels to renewable energy sources, especially wave and wind energy. The marine environment is a huge source of renewable energy that is being rapidly exploited. Among marine renewable energy technologies, offshore wind power stands out, combining three unique features: rapid technological development, inexhaustible energy source, and low construction costs [1,2].

The main advantage offered by the marine compared to the continental environment is that the prevailing winds are generally stronger and less variable, thus allowing the output of a floating wind turbine to be constant and, therefore, more efficient over time. In recent years, the scientific community has turned to the installation of floating structures in deep water utilizing the technology of floating wind turbines based on forms of floating structures that have been used in the extraction of oil and natural gas in deep water, such as floating semi-submerged [3], tension-leg platforms [4], etc.

Analysis of the wind conditions at the installation sites is necessary to model the operating environmental conditions of the floating structure. In this paper, the design values were estimated by applying a suitable bivariate model to describe wind speed and wave height and thus a common description of their extreme values. The frequency of occurrence of each sea state (Hs–Tp) was considered as a determining factor for the final calculation of the absorbed power in a certain period [5].

2. Materials and Methods

2.1. Floating System Properties

The floating system is set for the IEA 15 MW Reference Wind Turbine (WT). Detailed data are given in [6,7]. The floating platform consists of one central and three outer cylinders, which are attached to the WT tower. The structural parts of the structure are connected by smaller diameter cylindrical members (grey-colored members in Figure 1a). The draft of the floating structure is 20 m (Figure 1b).

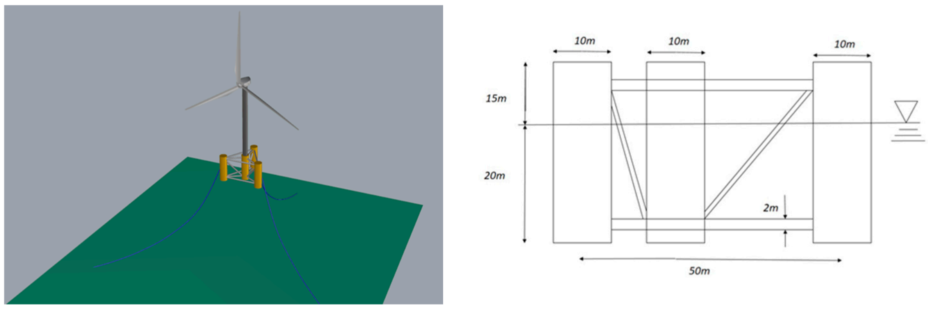

(**a**) (**b**)

Figure 1. (**a**) Three-dimensional representation of the floating system; (**b**) front view of the floating platform.

The floating platform has a displacement of 7203.352 t. The floating platform's center of mass (CM) is situated 2.543 m below sea water level (SWL), along the platform's centerline. The floating platform's roll, pitch, and yaw inertia are all equal at 5.169×10^6 tm^2 and 7.601×10^6 tm^2, respectively. The WT has a 2072 t total mass. The tower weighs 860 t and has a total height of 150 m. The Rotor Nacelle Assembly (RNA) has a mass of 1017 t. The three blades have a combined mass of 65 t and a length of 117 m without the hub [6].

2.2. Mooring System

There are three uniform mooring lines (87 mm R4-RQ4, Studless Chain, Steel) that make up the multi-leg catenary mooring system. The floating platform's three mooring lines run radially outward from the three outer cylinders and are connected to them at 120° angles. The fairlead locations are thought to be 14 m deep, while the water depth is 200 m. Each mooring line is 850 meters long and weighs 151 kg/m. Table 1 provides the anchor and fairlead positions in relation to the general inertial frame of reference.

Table 1. Mooring lines fairlead and anchor points.

Mooring Line Number	Fairlead (x, y, z) [m]	Anchor (x, y, z) [m]
Line 1	−16.934, −29.330 −14.000	−427.034, −739.644, −200.000
Line 2	−16.934, 29.330, −14.000	−427.034, 739.644, −200.000
Line 3	33.868, 0.000, −14.000	854.068, 0.000, −200.000

2.3. The ANSYS-AQWA Software

The potential flow theory is used in this study's numerical modeling, which is carried out using the ANSYS-AQWA software [8]. By assuming incompressible (non-viscous) and irrotational, the velocity potential is obtained:

$$\varphi = \varphi_I + \varphi_D \tag{1}$$

where

φ_D is the diffraction potential of the waves around the floating structure;
and
φ_I is the incident undisturbed wave potential.

By resolving the Laplace equation, applying the proper boundary conditions, and then calculating the pressure and ensuing forces acting on the structure, the potential function can be calculated.

The number of diffracted elements used in this study is 14,102, with a maximum element size of 2.5 m.

Hydrodynamic Loads

According to [9,10], the hydrodynamic loads are given:

$$F_j = -\iint_{S_B} p n_j dS \quad (2)$$

where p is the fluid pressure as determined by Bernoulli's equation, written as:

$$p = -\rho \frac{\partial \Phi}{\partial t} = -i\omega\varphi e^{-i\omega t} \quad (3)$$

where φ is the velocity potential.

For different wave headings (0–90 degrees), the numerical results for the horizontal wave loads Fx on the floating structure versus the wave frequency ω (rad/s) are displayed in Figure 2. The amplitude of the wave is H/2. Due to the platform's symmetry, it has been noted that the first-order wave excitation forces are equal for 60° and 120° wave heading, and for 30° and 150° wave heading. It is also concluded that the wave direction significantly affects the shape of the surge excitation force because of the hydrodynamic interaction between the floating platform's four cylinders under various wave conditions.

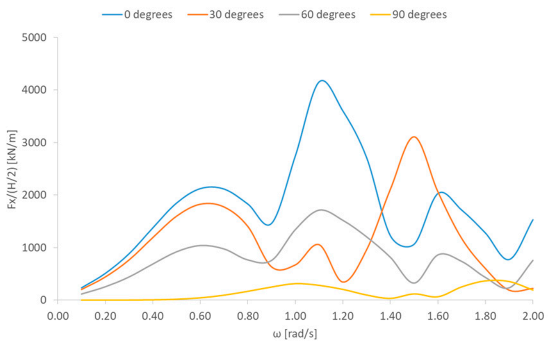

Figure 2. Fx horizontal wave loads for various wave headings (0–90 degrees) versus ω (0–2 rad/s).

3. Environmental Conditions

The design environmental parameters for a location in the Mediterranean basin are presented in this section. The water depth in the study area is about 200 m, coordinates 35.34° S, 26.80° E, and is located between Crete and Kasos.

The ECMWF's (European Center for Medium-Range Weather Forecasts) Era-20C dataset was used to generate numerical model simulation results for this region [11]. The initial simulations cover 111 years, from 1900 to 2010. Data from the years 1980 through 2010 covering the most recent 31 years of time series were examined [12,13]. The recording interval for the time series of characteristic wind and wave values is 3 hours. More details on the environmental analysis can be found in [5].

The data of significant wave height and peak period and their appearances in time form the Hs–Tp frequency table (see Table 2) and the area's most prevalent sea state can be characterized. The most frequent Hs–Tp value pair is (0–1 m, 4–5 s).

Table 2. Hs–Tp frequency table for the examined location.

Peak Period (s)	Significant Wave Height (m)						
	0–1	1–2	2–3	3–4	4–5	5–6	6–7
2–3	221	0	0	0	0	0	0
3–4	6702	7	0	0	0	0	0
4–5	24,291	1634	0	0	0	0	0
5–6	18,937	11,619	41	0	0	0	0

Table 2. *Cont.*

Peak Period (s)	Significant Wave Height (m)						
6–7	6869	11,028	1498	1	0	0	0
7–8	462	2492	2328	223	1	0	0
8–9	100	463	747	517	30	0	0
9–10	24	58	76	121	57	7	0
10–11	0	9	8	5	3	3	0
11–12	0	1	1	0	0	0	0

Operational Conditions

Having calculated the first-order exciting wave forces of the floating structure as a result of the presence of harmonic waves at different incidence angles (see Section 2), the first-order exciting wave force response spectra are obtained, i.e.,

$$S_i\,(\omega) \;=\; (F_i)^2 S_\zeta\,(\omega) \tag{4}$$

where i indicates the degree of freedom (i = 1: surge,), S_i is the response spectrum and S_ζ is the wave spectrum.

The significant values of the response spectrum are:

$$F_{i(\frac{1}{3})} = 2\sqrt{\int_0^\infty S_i\,(\omega) d\omega} \tag{5}$$

The maximum values of the response spectrum are 1.86 times higher than the significant values [9,10].

Table 3 shows the significant values for the first-order exciting wave forces (in kN) of the floating structure, for wave heading 0 degrees, applying the Jonswap spectrum with γ = 1 [10]. The largest of the significant values displayed in the table is 6150 kN (Hs–Tp: 5–6 m, 9–10 s).

Table 3. Significant values for the first-order exciting wave forces (in kN).

Peak Period (s)	Significant Wave Height (m)						
	0–1	1–2	2–3	3–4	4–5	5–6	6–7
2–3	47						
3–4	246	738					
4–5	473	1418					
5–6	612	1835	3058				
6–7	628	1883	3138	4393			
7–8	602	1805	3008	4211	5414		
8–9	578	1733	2888	4043	5198		
9–10	559	1677	2796	3914	5032	6150	
10–11		1619	2698	3777	4856	5935	
11–12		1555	2592				

4. Annual Wind Energy

The amount of energy that the under-study device with the 15 MW WT can produce in actual sea conditions is calculated in this section. To estimate the typical operating circumstances for offshore WT at the investigated location, the results shown in Table 3 will be further elaborated. Additionally, a study was conducted regarding the power that the WT absorbs for a variety of different wind speeds and the corresponding most likely sea states (see Table 4). Ref. [14] contains additional information. Moreover, we calculated the amount of absorbed wind power over wind speed using [6] for the absorbed power for the 15 MW WT.

Table 4. Most probable values of Hs–Tp and sub-sample size for various bins of the wind speed at the examined location and calculations of the absorbed power from the 15 MW WT.

Subsample Size	17,292	24,182	24,565	15,133	6527	2175	621	89
U_W (m/s)	2–4	4–6	6–8	8–10	10–12	12–14	14–16	16–18.62
H_S (m)	0.548	0.709	0.944	1.576	1.886	2.488	3.116	3.994
T_P (s)	3.777	3.792	4.906	4.906	6.256	6.914	7.573	8.331
Wind Power (MW) [6]	0.0	1.4	4.0	8.7	15.0	15.0	15.0	15.0
Final Absorbed Power (MWh/yr)	62.2	3174.8	9572.7	12708.9	9474.7	3157.3	901.5	129.2

After calculating the absorbed wind power of the WT for the specific sea area, the annual produced energy (in MWh) was determined, via extrapolation of the historical wind-wave data to a one-year period, while maintaining contribution ratios (time of occurrence) of each data (wave/wind) pair specific for the location. The results can be found in Table 4. Figure 3 shows the distribution of the absorbed power, for different wind speed values in the examined location.

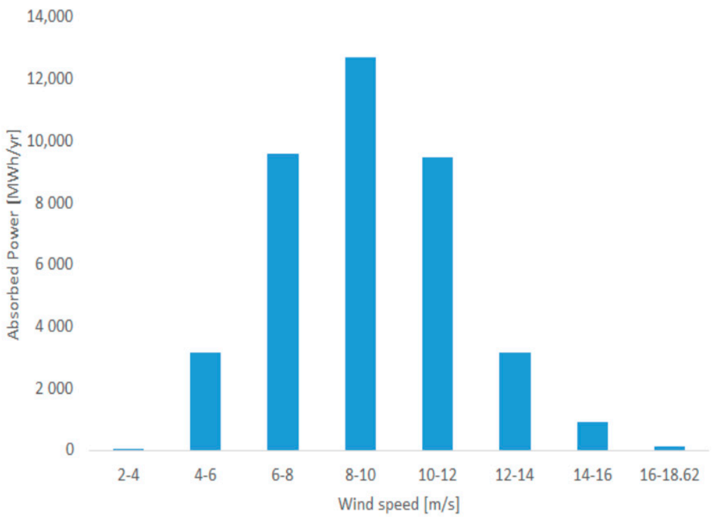

Figure 3. Absorbed Power from the 15 MW WT.

5. Discussion and Conclusions

A semisubmersible offshore structure with a catenary mooring system, supporting the IEA 15 MW Reference WT, has been presented. A frequency domain method has been used to calculate the system's exciting wave forces. Additionally, the significant first-order forces of the system have been calculated using a Jonswap spectrum for the irregular waves. Using wave hind-cast data between the Mediterranean islands of Crete and Kasos, the annual wind energy has been calculated.

The study reached the following conclusions:

1. The most frequently occurring sea state is characterized by the pair Hs = 0–1 m and Tp = 4–5 s.
2. The largest value of significant excitation wave force Fx is 6150 kN and corresponds to the pair (Hs–Tp: 5–6 m, 9–10 s), for wave heading 0 degrees (Table 3).
3. The 15 MW WT floating structure absorbs wind energy equal to 39,181 MWh/year.

The development of technology for the exploitation of green energy sources requires the interdisciplinary cooperation of various scientific fields, to become more targeted and, therefore, more efficient. The optimization of floating wind turbines and their support structures will give great impetus to the development of alternative energy sources. In this direction, the effort to utilize this inexhaustible energy resource will continue to be an area of further scientific investigation in the coming years.

Funding: This research received no external funding.

Institutional Review Board Statement: Not applicable.

Informed Consent Statement: Not applicable.

Data Availability Statement: Not applicable.

Conflicts of Interest: The author declares no conflict of interest.

References

1. Soukissian, T.H.; Denaxa, D.; Karathanasi, F.; Prospathopoulos, A.; Sarantakos, K.; Iona, A.; Georgantas, K.; Mavrakos, S. Marine Renewable Energy in the Mediterranean Sea: Status and Perspectives. *Energies* **2017**, *10*, 1512. [CrossRef]
2. Kardakaris, K.; Boufidi, I.; Soukissian, T. Offshore Wind and Wave Energy Complementarity in the Greek Seas Based on ERA5 Data. *Atmosphere* **2021**, *12*, 1360. [CrossRef]
3. Mazarakos, T.P.; Manolas, D.I.; Mavrakos, S.A. Design and Hydro-aero-elastic Modeling of a Multi Leg Mooring Concept for Floating Wind Turbine Applications. In Proceedings of the Sixteenth International Conference on Ecological Vehicles and Renewable Energies (EVER' 2021), Grimaldi Forum, Monaco, 5–7 May 2021.
4. Mazarakos, T.P.; Tsaousis, T.D.; Mavrakos, S.A.; Chatjigeorgiou, I.K. Analytical Investigation of Tension Loads Acting on a TLP Floating Wind Turbine. *J. Mar. Sci. Eng.* **2022**, *10*, 318. [CrossRef]
5. Mazarakos, T.P.; Mavrakos, S.A.; Soukissian, T. Energy Yield of a Floating Hybrid Mooring Wind Turbine System in the Aegean Sea. In Proceedings of the Fifteenth International Conference on Ecological Vehicles and Renewable Energies (EVER' 2020), Grimaldi Forum, Monaco, 10–12 September 2020.
6. Evan, G.; Rinker, J.; Sethuraman, L.; Zahle, F.; Anderson, B.; Barter, G.; Abbas, N.; Meng, F.; Bortolotti, P.; Skrzypinski, W.; et al. *Definition of the IEA 15-Megawatt Offshore Reference Wind*; NREL/TP-5000-75698; National Renewable Energy Laboratory: Golden, CO, USA, 2020. Available online: https://www.nrel.gov/docs/fy20osti/75698.pdf (accessed on 20 February 2023).
7. Christopher, A.; Viselli, A.; Dagher, H.; Goupee, A.; Gaertner, E.; Abbas, N.; Hall, M.; Barter, G. *Definition of the UMaine VolturnUS-S Reference Platform Developed for the IEA Wind 15-Megawatt Offshore Reference Wind Turbine*; NREL/TP-5000-76773; National Renewable Energy Laboratory: Golden, CO, USA, 2020. Available online: https://www.nrel.gov/docs/fy20osti/76773.pdf (accessed on 20 February 2023).
8. ANSYS. *Aqwa User Manual; Release 2022 R1*; ANSYS, Inc.: Canonsburg, PA, USA, 2022.
9. Faltinsen, O.M. *Sea Loads on Ships and Offshore Structures*; Ocean Technology Series; Cambridge University Press: Cambridge, UK, 1992.
10. Mazarakos, T.P. Second-Order Wave Loading and Wave Drift Damping on Floating Marine Structures. Ph.D. Thesis, School of Naval Architecture and Marine Engineering, Division of Marine Structures, Laboratory of Floating Structures and Mooring Systems, National Technical University of Athens, Athens, Greece, 2010. [CrossRef]
11. European Centre for Medium-Range Weather Forecasts. 2014, Updated Daily. ERA-20C Project (ECMWF Atmospheric Reanalysis of the 20th Century). Research Data Archive at the National Center for Atmospheric Research, Computational and Information Systems Laboratory. Available online: http://doi.org/10.5065/D6VQ30QG (accessed on 10 June 2015). [CrossRef]
12. Coles, S. *An Introduction to Statistical Modelling of Extreme Values*; Springer Series in Statistics; Springer: London, UK, 2001.
13. Soukissian, T.H.; Kalantzi, G. Extreme value analysis methods used for wave prediction. In Proceedings of the 16th International Offshore and Polar Engineering Conference, San Francisco, CA, USA, 28 May–2 June 2006.
14. Mazarakos, T.P.; Mavrakos, S.A. Mean Second Order Wave Drift Forces Contour of a Floating Structure Concept for Wind Energy Exploitation. In Proceedings of the 4th International Conference on Renewable Energies Offshore (RENEW 2020), Lisbon, Portugal, 12–15 October 2020.